Asymmetric changes of temperature in the Arctic during the Holocene based on a transient run with the CESM

Hongyue Zhang[1,2], Jesper Sjolte[2,*], Zhengyao Lu[3], Jian Liu[1,4,5,*], Weiyi sun[1], Lingfeng Wan[6]

[1] Key Laboratory for Virtual Geographic Environment, Ministry of Education, State Key Laboratory Cultivation Base of Geographical Environment Evolution of Jiangsu Province, Jiangsu Center for Collaborative Innovation in Geographical Information Resource Development and Application, School of Geography Science, Nanjing Normal University, Nanjing 210023, China
[2] Department of Geology – Quaternary Science, Lund University, Lund, 223 62, Sweden
[3] Department of Physical Geography and Ecosystem Science, Lund University, Lund, 223 62, Sweden
[4] Jiangsu Provincial Key Laboratory for Numerical Simulation of Large-Scale Complex Systems, School of Mathematical Science, Nanjing Normal University, Nanjing 210023, China
[5] Open Studio for the Simulation of Ocean-Climate-Isotope, Qingdao National Laboratory for Marine Science and Technology, Qingdao 266237, China
[6] Institute of Advanced Ocean Study, Ocean University of China, Qingdao, China

Correspondence to: Jesper Sjolte (jesper.sjolte@geol.lu.se), Jian Liu (jliu@njnu.edu.cn)

Abstract. The Arctic temperature changes are closely linked to midlatitude weather variability and extreme events, which has attracted much attention in recent decades. Syntheses of proxy data from poleward of 60°N indicate that there was asymmetric cooling of -1.54 °C and -0.61 °C for Atlantic Arctic and Pacific Arctic during the Holocene, respectively. We also present a similar consistent cooling pattern from an accelerated transient Holocene climate simulation based on the Community Earth System Model. Our results indicate that the asymmetric Holocene Arctic cooling trend is dominated by the winter temperature variability with -0.67 °C cooling for Atlantic Arctic and 0.09 °C warming for Pacific Arctic, which is particularly pronounced at the proxy sites. Our findings indicate that sea ice in the North Atlantic expanded significantly during the late Holocene, while a sea ice retreat is seen in the North Pacific, amplifying the cooling in the Atlantic Arctic by the sea ice feedback. The positive Arctic dipole pattern, which promotes warm southerly winds to the North Pacific, offsets parts of the cooling trend in Pacific Arctic. The Arctic dipole pattern also causes sea ice expansion in the North Atlantic, further amplifying the cooling asymmetry. We found that the temperature asymmetry is more pronounced in a simulation driven only by orbital forcing. The accelerated simulations lead to a partial delay in the feedback of climate processes. Therefore, we confirm the occurrence of the asymmetry of the Arctic temperature changes in unaccelerated simulations using ECBilt-CLIO, IPSL, and in Trace21k

1 Introduction

Arctic climate is a critical component of the climate system. Since the 1990s, the changes in the Arctic climate have attracted increasing attention. Observational and model data show that the Arctic temperature variability is much greater than the global mean temperature variability, known as the Arctic amplification (AA) (Jones and Moberg, 2003; Holland and Bitz, 2003;

Serreze and Barry, 2011). The Intergovernmental Panel on Climate Change (IPCC, 2021) suggests that the Arctic temperature has likely increased more than double compared to the global average with high confidence over the last two decades. There has been intense debate about how the AA affects the mid-latitude circulation, with some scholars suggesting that the AA increases the equator-to-pole temperature gradient and impacts the predominant westerly wind through the thermal-wind relation, which leads to disturbances in the mid-latitude circulation, further increasing the probability of extreme weather in the mid-latitudes (Smith et al., 2019; Vavrus, 2018; Screen and Simmonds, 2014; Cohen et al., 2014; Francis and Vavrus, 2012, 2015). The changes in Arctic temperature have also been directly linked to the sea ice loss or expansion, which affect the exchanges of heat and moisture between the ocean and atmosphere as well as the salinity of the ocean (Aagaard and Carmack, 1989; Wu et al., 2004; Goosse and Fichefet, 1999; Deser et al., 2016). Changes in sea ice extent and salinity in turn leads to changes in the thermohaline circulation (Rahmstorf, 1999; Alekseev et al., 2001), which may cause significant negative impacts on the climate and maritime transportation (Ragner, 2000) in high latitude regions. All these processes have strong impacts on the regional economic development.

The different drivers of the significant increase in temperature at high latitudes over the past decades have been debated by scholars, and it is widely accepted that one of the extremely important factors is the natural variability (Polyakov and Johnson, 2000; Polyakov et al., 2002; Delworth and Knutson, 2000). For the past decades, Hoerling et al. (2001) show that due to the increase in tropical temperature, convective activity has increased, resulting in an increase in the North Atlantic Oscillation/Arctic Oscillation (NAO/AO) positive pattern, which is significantly related with the Arctic temperature (Hurrell, 1995). (Deser et al., 2015; Blackport and Kushner, 2018) attribute part of the warming of the Arctic to increasing in extratropical ocean temperature. Johannessen et al. (2004) used ECHAM4 and HadCM3 and found that the anthropogenic forcing is the dominant reason for the Arctic warming over the past decades. For the centennial and millennial time scales, the anomalies in summer insolation, driven primarily by Earth's orbital forcing, have a greater impact on the Arctic region than the low latitudes and amplify changes in temperature through positive feedbacks. Many scholars proposed a link between Arctic temperature trends and summer insolation changes, especially during the early-mid Holocene (Park et al., 2018; Marcott et al., 2013; Kaufman et al., 2009). Arctic temperature change affects the radiative balance, which dominates the surface energy balance that controls Arctic sea ice growth and melting (Kay et al., 2008; Francis and Hunter, 2007). At the same time, sea ice changes and trends affect Arctic temperature through feedbacks and also influence Arctic atmospheric circulation changes, particularly in the lower troposphere during winter (Barnes and Screen, 2015; Overland and Wang, 2015; Francis and Skific, 2015; Cohen, 2016). The Holocene proxy data also suggest that a decrease in the Arctic sea ice relative to the present, impacting the temperature gradient between equator and pole, which might enhance warming in North American and North Pacific regions, leading to a slight decrease in temperature over East Asia, and shifting tropical rainfall northwards (Smith et al., 2019; Park et al., 2018; Hanslik et al., 2010; Funder et al., 2011; Müller et al., 2012).

From a geological perspective the characterization of the Arctic temperature variability captured by observational data is only a small fraction of the history of climate variations. The short time period of the observed Arctic temperature change are not sufficient to represent the full range of its natural variability and to fully assess feedbacks about air-sea interactions, climate,

70 and ecosystems, it is still necessary to study the long-term changes, especially the millennium-scale changes, which can help shed more light on Arctic climate change in the future. For the past two millennia, temperature reconstructions (such as tree-ring, sediment and ice core records) from PAGES2k, and model data show a millennial cooling trend in the late Holocene, particularly in the Atlantic Arctic compared to the Pacific Arctic (Zhong et al., 2018). Zhong et al. (2018) presents that this cooling pattern was caused by both a weaker North Atlantic subpolar gyre and a stronger Aleutian low. The Holocene (past

75 11,700 years) shows millennial scale climate variations forced by changes in insolation due to orbital changes. The early-mid Holocene period is known as the Holocene thermal maximum (HTM) due to an average 5% increase in solar radiation compared to the present (Berger, 1978). The warm climate conditions were particularly pronounced at high latitudes in the early-to-middle Holocene, which is usually associated with the insolation forcing (Kaufman et al., 2004; Larsen et al., 2015; Gajewski, 2015; Briner et al., 2016; Renssen et al., 2012). Previous work examining the response to Arctic temperature change

80 has either focused only on the trend over the whole Arctic and neglected potential regional asymmetry, or used only reconstruction data. The asymmetry of temperature change in the Arctic throughout the Holocene period, however, is evident (Fig. 1), likely associated with responses of climate modes to external climate forcings. The uncertainty and the low spatial coverage of reconstruction in temperature changes from proxy data makes it difficult to fully understand the Arctic temperature changes during the Holocene.

85 To overcome these limitations, a more comprehensive view of climate system changes can be obtained by using model data studies for the Holocene. There are some transient simulations covering the Holocene with different prescribed have been done during the past decades. For example, TraCE-21ka (Liu et al., 2009)) is a transient simulation with resolution of 3.75°×3.75° for exploring the climate evolution since the LGM, based on Community Climate System Model version 3(CCSM3). Bader et al., (2020) used the Max Planck Institute Earth System Model (MPI-ESM) perform transient simulations spanning the period

90 from 8 ka BP until the 1850 to investigate the contradiction of temperature trend changes between reconstructed and model simulated. Braconnot et al., (2019) used the transient Holocene simulations based on IPSL ESM with prescribed vegetation, interactive phenology and interactive carbon cycle for exploring the climate changes coupling vegetation over the last 6000 years. In this study, the transient simulation performed by Community Earth System Model (CESM) with an acceleration factor of 10 and a recent compilation of temperature proxy data are used to investigate the characteristics of the regional

95 temperature changes in the Arctic. Numerous studies have shown that accelerated transient simulations have the ability to study climate evolution over long time scales. For instance, Varma et al., (2012) compared the simulation results with 10 times acceleration and non-acceleration, and found that there is no significant difference in the characteristics of global surface climate change. Timm and Timmermann, (2007) used the earth system model of intermediate complexity ECBilt-CLIO to simulate the climate since the Last Glacial Maximum (LGM) by 10 times acceleration, and compared the simulation results

100 without acceleration and found that the simulation results with 10 times acceleration reproduced well the large-scale trend of atmospheric temperature in the Holocene. Lu and Liu, (2019) found that the acceleration leads to suppressed and delayed responses mainly in the deep sea and has less robust effect on the surface and subsurface. Jing et al., (2022) compared the temperature and precipitation changes in NNU-Holocene simulation and TraCE-21ka non-acceleration simulation, and in

terms of overall trend and distribution, the temperature and precipitation patterns of NNU and TraCE-21ka are similar. We are
105 therefore motivated to use these simulations to assess the changes in spatial pattern of Holocene Arctic temperature variability
and reveal the physical mechanisms behind these changes.

In this paper, we investigate whether temperature changes differed between the Atlantic and Pacific Arctic during the Holocene,
and whether changes in sea ice and sea level pressure contributed to the pattern of temperature changes. To address these
questions and identify the key factors driving asymmetric temperature changes, we analyze changes in sea ice, sea level
110 pressure, and orbital forcing from CESM NNU-Hol simulations and other transient simulations. This is critical for future
studies of the climate implications of temperature changes at high latitudes. The structure of this article is as follows. Sect. 2
describes the proxy and model data used in the current study. In Sect. 3, we summarized the temperature asymmetric changes
reflected in the proxy and model data in the high latitudes of the Northern Hemisphere and presented the changes in sea ice
and sea level pressure during the Holocene. In Sect. 4, the characteristics of Arctic temperature changes in Holocene
115 unaccelerated simulations are discussed. Finally, a summary is given in Sect. 5.

2 Method and data

2.1 The CESM Model and the transient simulations

This study analyzes a new transient simulation result based on the CESM, named NNU-Hol (Nanjing Normal University-
Holocene), which considers more comprehensive external forcings for the Holocene climate change. The CESM is a fully-
120 coupled, global climate model, which was launched by the National Center for Atmospheric Research (NCAR) in June 2010.
It is an Earth System Model developed on the basis of CCSM. The CESM includes components for atmosphere, ocean, sea
ice, as well as the land surface, and considers atmospheric chemistry, biogeochemistry, and anthropogenic forcing. It is widely
used to study the mechanism of the changes in climate and environment, the interaction between natural and anthropogenic
forcing for climate and for scenarios of future climate change . The CESM is coupled with several advanced modules, including
125 the CAM5 (Community Atmosphere Model 5) used by the atmosphere module, the POP2 (Parallel Ocean Program 2) used by
the ocean module, the CLM4 (Community Land Model 4) used by the land module, the CICE (The Los Alamos National
Laboratory Sea-ice Model) used by the sea ice module and the CISM2.0 (The Glimmer Ice Sheet Model 2.0) used by the land
ice module . The CISM2.0 is deactivated in the NNU-Hol simulation. For a more detailed introduction, please visit the official
website of CESM (http://www.cesm.ucar.edu/models/cesm1.0/notable_improvements.html).
130 In NNU-Hol, the CESM 1.0.3 was configured to simulate the transient climate evolution of the Holocene period at a horizontal
resolution of 3.75°×3.75°, forced by several external forcings (orbital parameters, solar irradiance, volcanic eruptions,
greenhouse gases, and land use/land cover) accelerated by a factor of 10. With this acceleration method (Lorenz and Lohmann,
2004), climate trends and feedbacks from the past 11.95 ka BP to 1990 AD, imposed by the external forcing driven changes,
are represented in the experiments with 1199 model years to save computation resources. The solar irradiance forcing comes
135 from the reconstruction of (Vieira et al., 2011), aggregated to 10-year average timescale of solar forcing and prescribed into

the simulation. The volcanic eruption comes from the ice core based reconstructions of (Gao et al., 2022) and (Sigl et al., 2015). For the volcanic forcing, the volcanic events during the 10-year period were integrated into one volcanic eruption event. On the basis of this assumption, the horizontal diffusion of lower stratospheric aerosols was calculated using the stratospheric transport parameters. Based on the stratospheric-tropospheric folding and BD (Brewer Dobson) circulation theory latitude-

140 and time-dependent functions to describe aerosol production and deposition (Grieser and Schonwiese, 1999; Holton et al., 1995). The greenhouse gas forcing data uses the reconstruction based on ice cores in (Joos and Spahni, 2008). The data of land use/extra-land cover forcing comes from the HYDE 3.2.1 (the History Database of the Global Environment, referred to as HYDE version 3.2.1) (Goldewijk et al., 2017) data set. The orbital parameters come from Berger (1978). The external forcing timeseries used in the NNU-Hol simulation is shown in the supplementary material. Wan et al. (2020) found that the global

145 annual average temperature in the NNU-Hol All forcing simulation and reconstruction records from Marcott et al. (2013) has similar trends and strengths, decreasing about 0.5 K during 5.0 to 0.15 ka BP. We explore the characteristics of changes in Arctic temperature during the Holocene and try to understand its underlying mechanism based on the All forcing (AF) and orbital forcing (ORB) simulations in NNU-Hol.

There are, to our knowledge, 5 sets of climate simulations published so far covering the entire Holocene period (0-11700 ka

150 BP), namely ECBilt-CLIO (Timm and Timmermann, 2007), FOAM (Kutzbach et al., 2008), TraCE-21ka (Liu et al., 2009), FAMOUS (Smith and Gregory, 2012) and LOVECLIM (Timmermann et al., 2014). Except for TraCE-21ka and one of the ECBilt-CLIO simulations, these simulations are accelerated by different factors. Additional unaccelerated simulations, such as the simulations based on MPI-ESM (Bader et al., 2020) and IPSL (Braconnot et al., 2019) covering only part of the Holocene period (0-8 ka BP and 0-6 ka BP respectively) have also been published in recent years. The external forcings considered in

155 these simulations are generally a part of the combination of the Orbital Forcing (ORB), the Greenhouse Gases (GHG), the continental ice sheets (ICE), the Meltwater Flux (MWF), the Volcanic Forcing, the Landuse Forcing and Ozone Forcing.

2.2 Reconstructing Paleo Proxies data

In order to better understand the Holocene evolution of the earth system, a comprehensive database of paleoclimate records was compiled by Kaufman et al., (2020), which is named the Temperature 12k database.

160 Temperature 12k database is a global compilation of good-quality, published, temperature-sensitive proxy records (such as lake sediment, marine sediment, peat, glacier ice and pollen, etc) through the entire Holocene period. The data is mainly collected from previously published research, containing 1319 records (1162 from the Northern Hemisphere and 157 from the Southern Hemisphere), distributed in 679 sites (including 470 terrestrial and 209 marine sites) where time period cover at least 4000 years. For our study we only selected records with a resolution finer than 400 years, 15% of these records have a resolution

165 of 50 years or finer, 39% have a resolution of 51 to 150 years, and 21% have a resolution of more than 250 years.

The data is mainly based on a collection of published reconstructions of Holocene temperature especially in the Northern Hemisphere (Routson et al., 2019; Marcott et al., 2013; Sundqvist et al., 2014; Chen et al., 2008; Wanner et al., 2011). Part of the data collected the global paleotemperature records from PAGES 2k Consortium 9 database. The compilation of Marsicek

删除了：covering only part of the Holocene period

删除了：covering the Holocene

删除了：periods,

删除了：, respectively,

删除了：Some unaccelerated simulations have also been published in recent years, such as those covering the Holocene 8ka BP and 6ka BP based on the MPI-ESM (Bader et al., 2020) and IPSL (Braconnot et al., 2019), respectively.

et al., (2018) provides most pollen-based paleotemperature records and the other part comes from public repositories (such as PANGAEA and World Data Service for Paleoclimatology, NOAA). The paleotemperature records in 209 marine sites are mainly from the US-based Data Assimilation for Deep Time (DADT) project and the compilations of the German Climate
180 Modeling Initiative (PalMod) (Jonkers et al., 2020). In this database, uncertainties are estimated by various methods. Some studies characterize uncertainty based on calibration and proxy bias, or measurement error, while others represent uncertainties after rigorous cross-validation. The uncertainties of most of these paleotemperature records from North American and European pollen and most of the marine sediment-based records (except for those from microfossil assemblages) are calculated using the Bayesian procedure in early studies (Malevich et al., 2019; Tierney and Tingley, 2014, 2018; Tierney et al., 2019).
185 For the other proxy types, most of the paleotemperature values and their uncertainties are based on multigenerational analysis and calibration methods. Specific information about the uncertainty for each proxy recorded is available in Kaufman et al., (2020) Supplementary Table 2 as well as in the original publication. More detailed information can be found at www.ncdc.noaa.gov/paleo/study/27330.

In order to investigate the changes in temperature over the Arctic area during the Holocene, we selected records from the site,
190 which are located above 60 degrees north latitude, and eliminated some records with shorter time series (missing more than 2500 years during the Holocene), which leaves us with 58 records.

2.3 Analytical and Statistical Methods

We focus on long-term temperature changes in the Arctic during the Holocene. The significance test used in this study was calculated according to the two-tailed Students t-test at the 90% (alpha = 0.1) or 95% (alpha = 0.05) confidence level. The
195 Students t-test was used to compare the means of two groups and determine if the difference in means is statistically significant and was also used to test the statistical significance for each grid point in the figures below. The sample size of the Pacific Arctic region in the temperature proxy data is small and thus a small degree of freedom. The potential impact of temporal and spatial correlation is not taken into account in the analyses. We apply empirical orthogonal function (EOF) analysis, also known as principal component analysis (PCA), to sea level pressure changes in the Northern Hemisphere. EOF analysis is a
200 standard analytical technique used in climate science to study patterns of spatial variability. EOF is obtained by computing the eigenvectors and eigenvalues of the spatially weighted covariance matrix of the temperature field. Applying EOF to the Northern Hemisphere sea level pressure is a common method to study the Arctic dipole mode. The objective is to show the variation of the Arctic dipole mode during different periods of the Holocene (0-2 ka BP, 5-8 ka BP). As described in Section 3 below, the second mod of EOF for the Holocene 5-8 ka BP period explains 11.5% and that for 0-2 ka BP period explains
205 16.3% of the sea level pressure variation.

删除了: of each grid

3 Result

3.1 Arctic Temperature Change
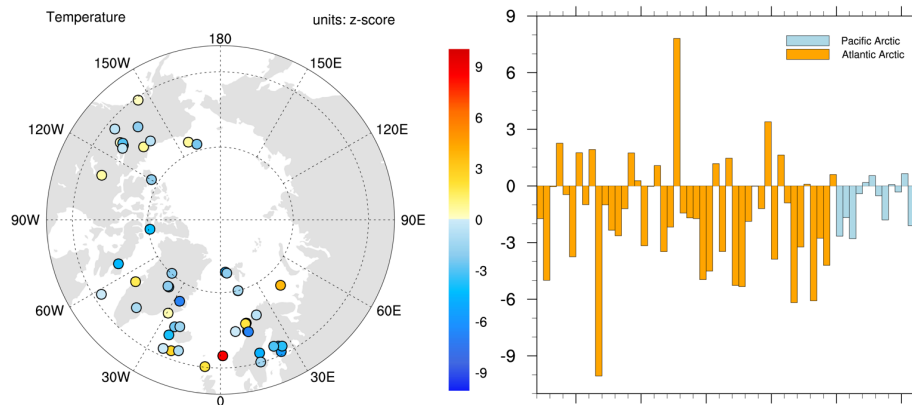
Figure 1: (a) The annual temperature changes between two period (0-2 ka BP minus 5-8 ka BP) in Reconstructions (Temperature 12k); (b) Histogram of temperature change for each proxy site

In order to demonstrate asymmetric temperature changes in the Arctic during the Holocene, we analyzed the Temperature 12k database (Kaufman et al., 2020). The results are shown in Fig. 1, where the circles represent the site locations of the 52 selected records. The proxy records are mainly concentrated on the Atlantic coast, Europe, Greenland, and northern Canada. The average temperature across the Arctic showed a cooling trend during the Holocene, which is consistent with previous findings (Marcott et al., 2013; Kaufman et al., 2004). To study the asymmetric changes in temperature, we divided the Arctic region into two parts, the Pacific Arctic (Lat > 60°N, Lon 90°W ~ 59°E) and the Atlantic Arctic (Lat > 60°N, Lon 60°E ~ 91°W). The proxy data shows that there is an asymmetric cooling between the two regions, with an average cooling of -1.54 °C in the Atlantic Arctic and -0.61 °C in the Pacific Arctic respectively, showing significance at the 90% confidence level (p<0.10) on students t-test. The degrees of freedom of the temperature proxy data in the Pacific and Arctic region is small. The histogram shows that only two proxy sites have extreme temperature variations in the Atlantic Arctic region. However, combined with the box plot of the temperature changes (Supplementary Fig. 1), the asymmetric temperature variation in the two regions is still considered robust. To further study the robustness of this asymmetric change in temperature, we likewise analyze it with model data, allowing us to also investigate the seasonal changes.
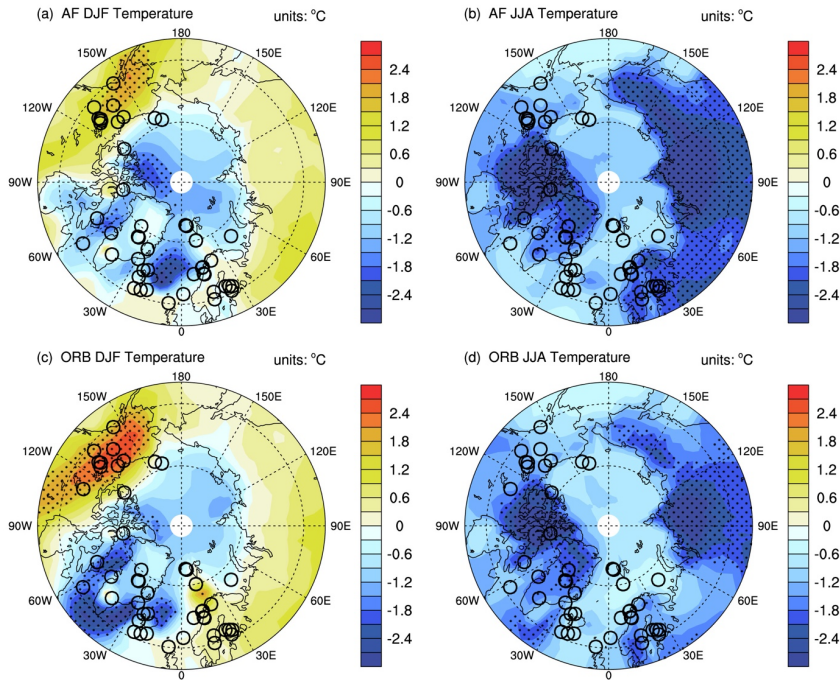
Figure 2: (a) The DJF temperature changes between two periods (0-2 ka BP and 5-8 ka BP) in NNU-Holocene All forcing simulations (Pacific Arctic:-0.44, Atlantic Arctic:1.00, the difference is statistically significant at the 95% confidence level); (b) Same as (a) but for JJA (Pacific Arctic:3.98, Atlantic:3.81) (c) Same as (a) but for NNU-Holocene ORB forcing simulations (Pacific Arctic:-0.80, Atlantic Arctic:1.75, the difference is statistically significant at the 95% confidence level); (d) Same as (c) but for JJA (Pacific Arctic:7.48, Atlantic Arctic:6.07). Areas that are dotted are significant at the 90% confidence level.
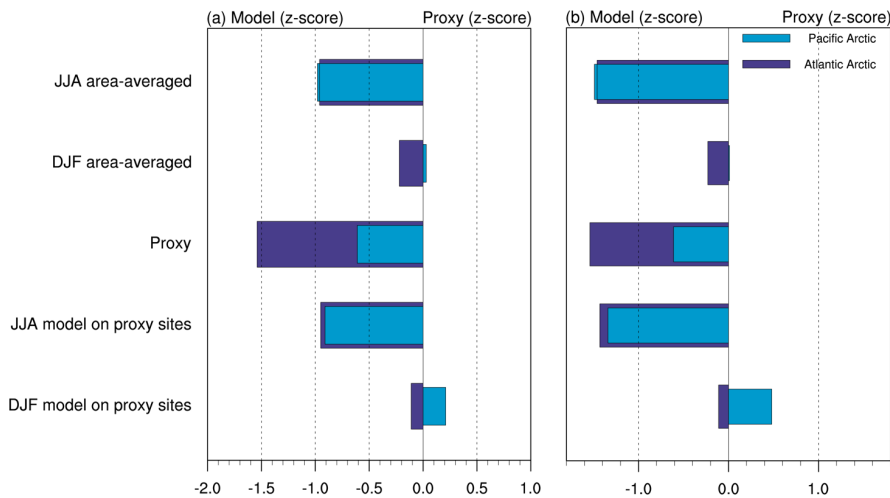
Figure 3: 1) Model area average temperature change in JJA; 2) Model area average temperature change in DJF; 3) Annual temperature change in Proxy; 4) Model JJA average temperature change on proxy sites; 5) Model DJF average temperature change on proxy sites (a: AF simulation, b: ORB simulation);

Here we use the model data based on the CESM, the NNU-Hol, and we choose data from All Forcing simulation (AF) and Orbital forcing simulation (ORB) in order to assess the most realistic temperature changes (AF) and the role of the orbital forcing (ORB) in the changes during the Holocene. As shown in Figure 2, to better understand the asymmetry, we further analyze the temperature changes in two seasons, DJF (December, January and February) and JJA (June, July and August). The results from AF and ORB show a similar pattern. In the JJA, the Artic exhibits a comparable cooling trend in the Atlantic sector and the North Pacific sector, with cooling centers in Eurasia and northeastern America. However, there is significant regional asymmetric cooling in the DJF (-0.67 °C for Atlantic Arctic average cooling and 0.09 °C for Pacific Arctic average warming in AF, the difference is statistically significant at the 95% confidence level on students t-test), with the Arctic Ocean, the North Atlantic Ocean and Greenland are cooling, while the land and North Pacific Ocean are warming. Areas that are dotted are significant at the 90% confidence level in Fig. 2. Northern Canada, where numerous proxy sites are located, is the center of the temperature warming, with the cooling center changing from the Straits in the AF to the North Atlantic in the ORB. We can see more clearly the difference of temperature asymmetry in two seasons through Figure 3, and the intensity of the asymmetry is more pronounced at the proxy sites. In the DJF of AF, the average cooling is -0.44 °C for the Atlantic Arctic proxy site and the average warming is 0.85 °C for the Pacific Arctic proxy site, while in the ORB it is -0.25 °C and 1.61°C, respectively. The difference in the mean temperature changes in the two regions is significant at the 90% confidence level in

both AF and ORB. Fig.3 shows that the temperature difference between the Pacific and Atlantic Arctic is neglectable for either the regional average or the sites station average in JJA. Therefore, the asymmetric temperature changes of the Atlantic and Pacific Arctic are dominated by the changes in DJF.

3.2 Sea Ice (March) and Sea Level Pressure Change

255
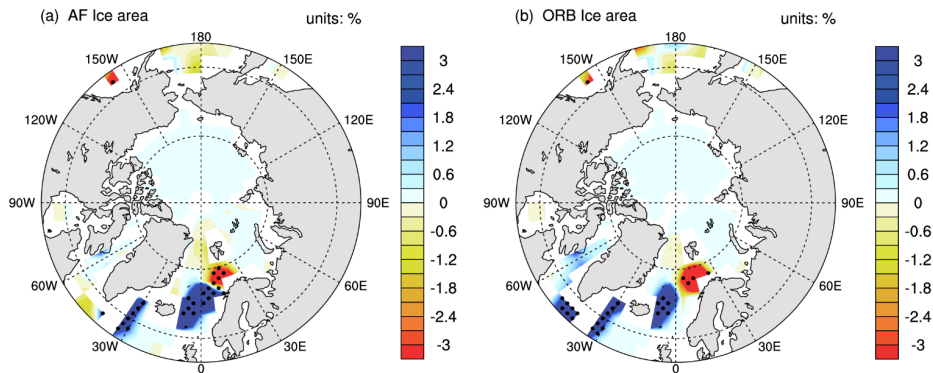
Figure 4: (a) The March sea ice area (aice) changes between two period (0-2 ka BP and 5-8 ka BP) in NNU-Holocene All forcing simulation (regional average on Pacific Arctic:0.02% and Atlantic Arctic:0.29%); (b) Same as (a) but for ORB forcing simulation (regional average on Pacific Arctic:0.04%, Atlantic Arctic:0.29%); Areas that are dotted are significant at the 90% confidence level.
260 **The difference of the means sea ice area changes in the two regions is significant at the 90% confidence level in both AF and ORB.**

The past research has shown that sea ice is always an important factor when we discuss Arctic climate change (Jenkins and Dai, 2021). Arctic temperature changes are often tightly linked to sea ice changes, with temperature causing changes in the expansion of sea ice cover and therefore changes in surface albedo, further amplifying climate change at Arctic region (Wohlfahrt et al., 2004; Renssen, H. et al., 2005; Braconnot et al., 2007). The simulations show that the temperature asymmetry
265 is closely related to the asymmetric change in sea-ice pattern. The difference in March sea ice area between the two periods (0-2 ka BP and 5-8 ka BP) is fairly consistent in the AF and ORB simulations. Consistent with previous studies of Holocene sea ice concentration proxy, sea ice concentrations were low in the early-mid Holocene and increased in the mid-late Holocene during the Neoglacial (Jennings et al., 2002; de Vernal et al., 2005; Müller et al., 2012). For the Atlantic Arctic, the sea ice concentration of Chukchi Sea was not always low during the Early Holocene, while there were millennial oscillations and
270 minimum values in the Chukchi Sea during the Neoglacial (de Vernal et al., 2005). Müller et al.,(2012)showed that for the North Atlantic sea ice reconstruction P25 decreased significantly in the early Holocene, while in the middle Holocene 7000-3000 years BC, sea ice gradually increased. The maximum value was gradually reached in 3000-300 years. In our model, sea

ice increased throughout the Arctic during the Holocene, especially around the Norwegian Sea and Davis Strait, with the exception of the Barents Sea, where sea ice area declined significantly (significant area are dotted in Fig. 4). The large expansion of sea ice in the North Atlantic and the slight decrease in sea ice in the North Pacific leads to strong differences in surface albedo between the two regions, with more reflection of radiation in the North Atlantic and more absorption in the North Pacific, which contributes to the stronger asymmetry during winter (Fig. 3).
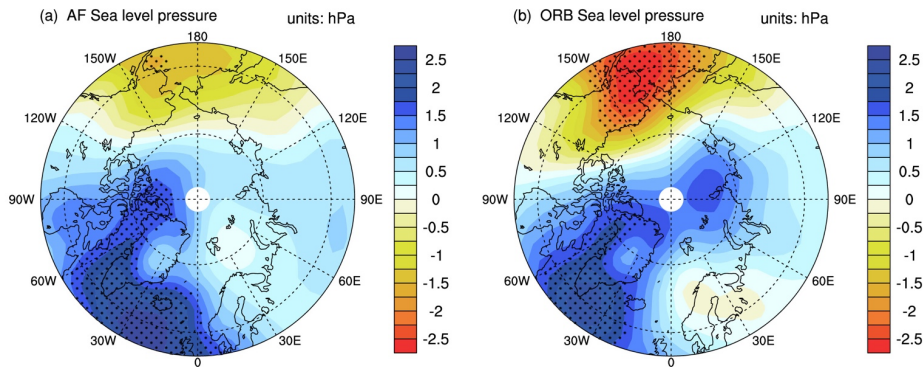
Figure 5: (a) The DJF sea level pressure changes between two period (0-2 ka BP and 5-8 ka BP) in NNU-Holocene All forcing simulation;(b)Same as (a) but for ORB forcing simulation; Areas that are dotted are significant at the 90% confidence level.

To understand the dynamical aspects of the stronger cooling in the North Atlantic, we investigate the regional-scale atmospheric circulation and surface wind variations related to sea-ice transport. We focus our analysis on the December–February season, because these months yield the largest impact of temperature asymmetry. In DJF, the sea level pressure (SLP) has a distinct dipole distribution. Sea level pressure increases in the North Atlantic and decreases in the North Pacific. The low pressure in the North Pacific is intensifying during the late Holocene. Based on data from the past decades, many studies (Wu et al., 2006; Niebauer et al., 1999; Stabeno et al., 2001; Rodionov et al., 2005) have demonstrated that the stronger low pressure transported warm air from the south to the North Pacific, resulting in higher temperatures in the North Pacific, offsetting parts of the Holocene cooling trend in the North Pacific and causing sea ice expansion in the North Atlantic due to atmospheric circulation. We suspect that this contributes to the regional asymmetry in Arctic temperatures. Compared with the AF results, the ORB simulation shows that the sea level pressure changes in the two regions are more contrasting and the difference is larger. This suggests that orbital forcing plays a dominant role in generating this asymmetry.

删除了: This suggests that orbital forcing plays a contributing role in generating this asymmetry more than other forcings

带格式的: 右

3.3 EOF of SLP and regressed UV wind and sea ice
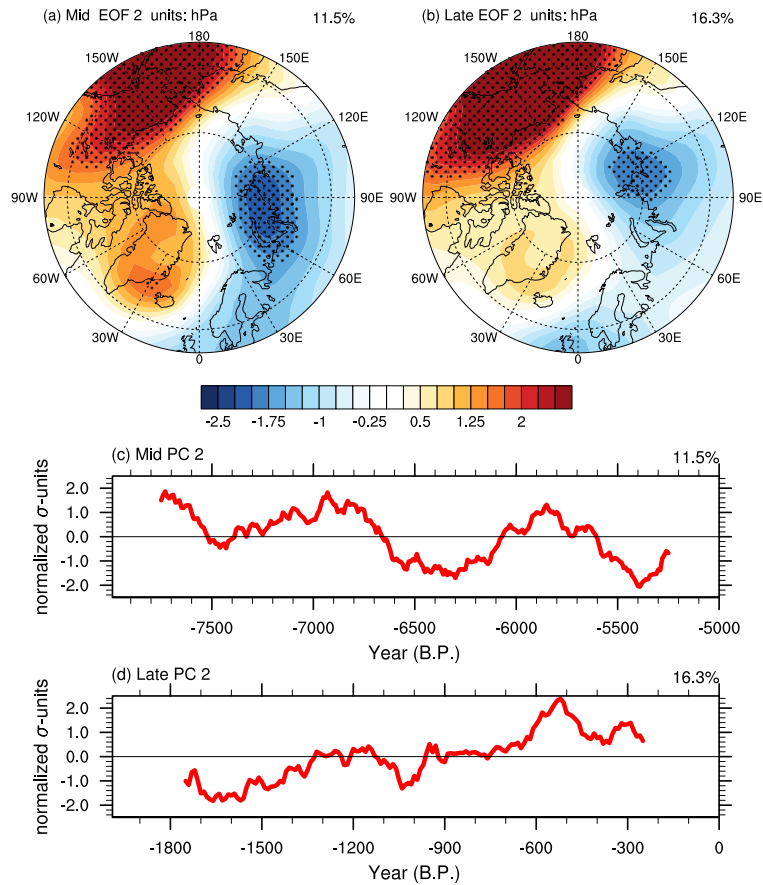
Figure 6: The second EOF (EOF2) pattern of the Sea level pressure in NNU-Holocene All forcing simulations during 5-8 ka BP (a) and 0-2 ka BP (b); The second Principal Component time series of the EOF during 5-8 ka BP (c) and 0-2 ka BP (d) after 50yr smoothed; Areas that are dotted are significant at the 90% confidence level.

Previous studies have established that atmospheric circulation anomalies in the Arctic atmosphere, dipole structure anomalies, are closely related to sea ice (Wu et al., 2006; Watanabe et al., 2006; Choi et al., 2019). The Arctic dipole strongly influences

sea ice movement and sea ice export. The empirical orthogonal function(EOF)method is commonly used to study the Arctic
305 dipole in past studies (Wu et al., 2006; Skeie, 2000; Wang and Ikeda, 2000). The EOF's first leading mode of the monthly
mean SLP north of 60 degrees north latitude in winter corresponds to the Arctic Oscillation pattern and the second leading
mode of the EOF corresponds the of the dipole anomaly. In order to confirm our conjecture that changes in SLP and sea ice
play a role in promoting regional temperature asymmetry, we analyzed the Arctic dipole, and the results are shown in Fig. 6.
The first and second leading modes are statistically independent at 95% confidence level. In the AF simulation, the EOF pattern

310 of the SLP is similar for both periods (0-2 ka BP and 5-8 ka BP), with the second mode showing an Arctic dipolar distribution.
There are two action centers with opposite signs one center is located over the North Pacific and the other exists over the
northern Eurasia (significant at the 90% confidence level), accounting for 11.5% (5-8 ka BP) and 16.3% (0-2 ka BP) of the
variance. Fig. 6c, d shows that the PC2 time series of the EOF in the mid-Holocene oscillated repeatedly, while the PC2 in the
late Holocene has shown a strengthening trend. Combined with the stronger SLP of the late Holocene shown in Fig. 5, it can
315 be known that the late Holocene has a stronger Arctic Dipole pattern.

Regressing on PC2 of EOF allows us to understand how the Arctic dipole pattern affects the changes in sea ice and wind, and
the corresponding sea ice field and wind field can explain the physical mechanism of the Arctic dipole effect on temperature
asymmetry. To explore our conjectures, we compared two spatial patterns of sea ice and UV wind field regressions to PC2
(Fig. 7). By regressing the sea ice distribution onto the second Principal Component time series (Fig. 7), a pattern is consistent
320 with past sea ice reconstructions (de Vernal et al., 2005; Müller et al., 2012; Jennings et al., 2002), we show that the Arctic
dipole in the late Holocene had a greater role in influencing sea ice. In the late Holocene, the Bering Strait, Chukchi seas and
East Siberia were influenced by warm winds from the south, promoting strong ice melting, pushing the ice away from the
coast and increasing the temperature in these areas. On the other hand, the pressure pattern causes the Arctic Ocean sea ice to
expand to the North Atlantic Ocean through Fram Strait transfer. This leads to more sea ice in the Atlantic Ocean, and therefore,
325 more radiant heat reflected and surface temperature cooling in Atlantic Arctic due to the sea ice feedback. This pattern
contributes to the asymmetry of temperature variations between the North Atlantic and the North Pacific. In the late Holocene,
the wind field characteristics are more pronounced than those in the early-mid Holocene, and thus the temperature asymmetry
is more significant.
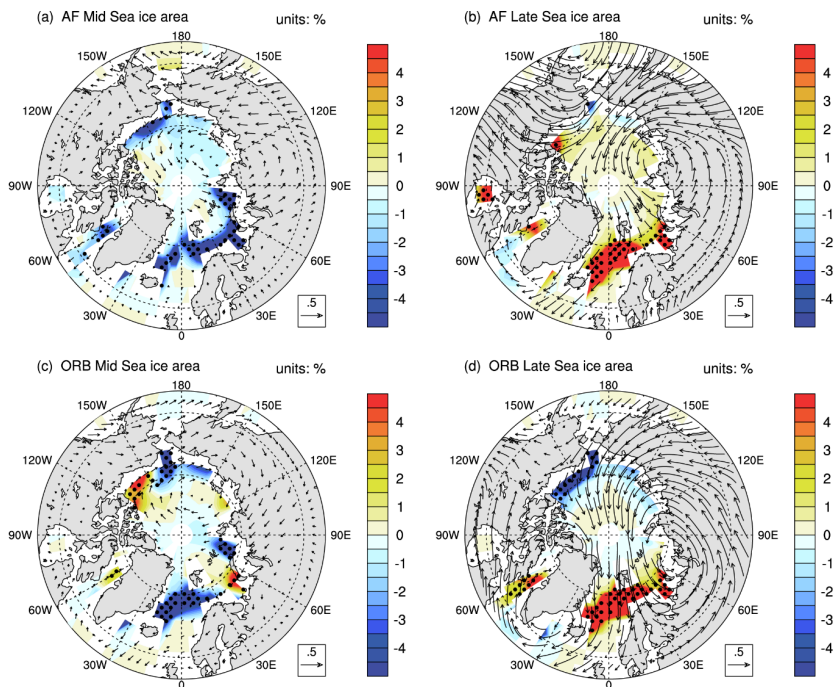
330

Figure 7: The regression of UV wind and sea ice based on the second Principal Component time series of the Sea level pressure in NNU-Holocene AF simulation during 5-8 ka BP (a) and 0-2 ka BP (b); in the NNU-Holocene ORB simulation during 5-8 ka BP (c) and 0-2 ka BP (d); Areas that are dotted are significant at the 90% confidence level.
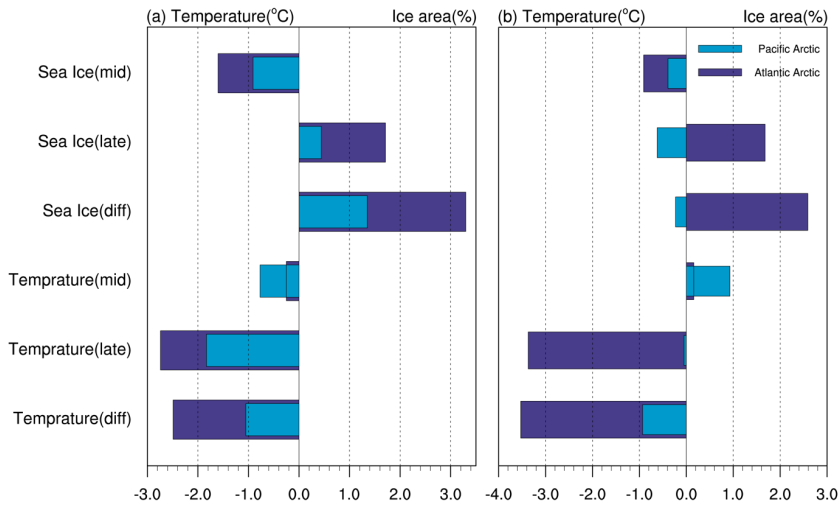
Figure 8: 1) Average change in the regression of Sea ice on the PC2 of the SLP in early-mid Holocene; 2) same as 1) in late Holocene; 3) Differences in the regressions of Sea ice on PC2 of SLP between two period; 4) The regression of temperature average change in early-mid Holocene; 5) same as 4) in late Holocene; 6) Differences in the regressions of temperature on PC2 of SLP between two period (a: AF simulation, b: ORB simulation); the difference in sea ice and temperature between two period are statistically significant at the 90% confidence level.

Figure 8 shows the average change in the regression of temperature and sea ice onto PC2, and the differences in sea ice and temperature between the two regions are mainly contributed by the Late Holocene period. The regression of sea ice on the PC2 of SLP increased by 1.71% in North Atlantic and 0.44% in North Pacific during the late Holocene, while decreased by -1.60% and -0.91% during the early-mid Holocene (significant at the 90% confidence level). The corresponding asymmetric cooling in the early-mid to late Holocene was -2.74°C in the North Atlantic and -1.83°C in the North Pacific (significant at the 90% confidence level). The results of the ORB simulations in terms of asymmetry are similar to the AF simulations, but stronger. Figure 7 shows that in the ORB simulation, the late Holocene had stronger warm southerly winds and more open water in the North Pacific, while sea ice expanded more widely in the North Atlantic, resulting in stronger asymmetric temperature. The regression of temperature shows a cooling of -3.37°C and -0.05°C in the North Atlantic and North Pacific(significant at the 90% confidence level), respectively, during the late Holocene. Therefore, the regression of the UV wind, the sea ice and the temperature on PC2 show the contribution of the Arctic Dipole to the temperature asymmetry, The result indicating that it is an important factor affecting the temperature asymmetry in the Arctic.

4 Discussion

The results indicate that the sea level pressure and sea ice changes are an important factor for the asymmetric Arctic cooling, since these two factors show similar asymmetric variations over the North Atlantic and the North Pacific. Compared with the early-mid Holocene, the sea ice expanded in the North Atlantic during the late Holocene, which leads to more cooling in the Atlantic Arctic due to its feedback. On the other hand, the Arctic dipole pattern, which plays an important role in sea-ice expansion in the North Atlantic, promotes more cooling in Atlantic Arctic and raising the temperature in the Pacific Arctic with warm southerly winds, exacerbating the temperature asymmetry. The asymmetric pattern is consistent with the asymmetric cooling in the Arctic over the past 2,000 years (Zhong et al., 2018). (Zhong et al., 2018) suggests that the change in ocean density due to the millennial cooling has led to a slowdown of the subpolar circulation. This deceleration of the subpolar circulation reduces the heat advection in the northern North Atlantic and intensifies the cooling in Atlatntic Arctic region. Our results are qualitatively consistent with their results that sea level pressure and sea ice play an important role in the asymmetric cooling. However, it should be pointed out that meltwater forcing was not prescribed in NNU-Hol, thus the response in ocean salinity and subpolar circulation as Zhong et al. (2018) due to meltwater can be underestimated in our simulation.

It can be assumed that our accelerated simulations are largely in qualitative agreement with the unaccelerated experiments in terms of the long-term climate evolution without involving changes in the deep ocean. We present some simple results to validate our results by comparing other non-accelerated simulations. We have selected three open-access unaccelerated simulations, TraCE-21ka, ECBilt-CLIO and IPSL. The ECBilt-CLIO is an Earth System Model of Intermediate Complexity.

In summary, for the asymmetric cooling of the Arctic, the simulations of ECBilt-CLIO as well as IPSL are similar to our results, while TraCE-21ka differs from our results. In particular, both ECBilt-CLIO and IPSL simulations show asymmetric cooling in the two Arctic regions and both have a greater cooling in the North Atlantic than in the North Pacific. The first transient simulations (Timm and Timmermann, 2007) based on the ECBilt-CLIO model with a horizontal resolution of about 5.6° × 5.5° and covering the past 21 ka, with the external forcing of ice cover, greenhouse gas concentration, and orbital configuration. The unaccelerated simulations using ECBilt-CLIO similarly reveal a regional asymmetry in temperature variability during the early-mid to late Holocene, with greater cooling in the North Atlantic (-0.26 °C cooling) than in the North Pacific (-0.02 °C cooling) (significant at the 90% confidence level; Supplementary Fig. 3). The second nonaccelerated simulations based on IPSL ESM model (Braconnot et al., 2019) explored the relationship between climate change and vegetation over the past 6000 years. The IPSL ESM also captures the asymmetry characteristics of Arctic temperature variability between the mid Holocene (4-6ka BP) and late Holocene (0-2 ka BP),with -0,14 °C cooling in the Pacific Arctic and -0.18 °C cooling in the Atlantic Arctic (Supplementary Fig. 3). However, the result of IPSL did not significant. The asymmetric changes are more pronounced if we focus only on the North Atlantic and North Pacific ocean regions. However, the results of TraCE-21ka are slightly different. TraCE-21ka is forced by the Earth's orbital parameters forcing, the greenhouse gas forcing, the meltwater flux forcing, and the continental ice sheets forcing. Its results show that the difference in annual

385 mean temperature between the early-mid Holocene and late Holocene is significantly cooler in the Arctic and there is a regional asymmetry in temperature changes between the two regions, with -0,94 °C cooling in the Pacific Arctic and -0.06 °C cooling in the Atlantic Arctic (significant at the 90% confidence level; Supplementary Fig. 3). However, unlike NNU-Hol, the cooling in the Atlantic Arctic is smaller in magnitude than that in the Pacific Arctic in the asymmetric change of temperature in TraCE-21ka. This result might be attributed to the different external forcings of TraCE-21ka and NNU-Hol: there is still considerable

390 residual ice-sheets and freshwater discharge in TraCE-21ka at about 8 ka BP which is not present in NNU-Hol.

Earlier work was more focused on the effects of the Arctic amplification in recent decades. Based on the observation data, it is assumed that AA will further increase the possibility of extreme weather in mid-latitude regions by increasing the temperature gradient from the equator to the pole in dynamic ways. However, the mechanism behind this is still not fully understood (Xue et al., 2017; Cohen et al., 2018; Chen et al., 2015; Vavrus, 2018; Screen, 2017). For long-term Arctic climate

395 research, it is mainly the study of temperature trend changes based on reconstructed proxy data (Kaufman et al., 2004; Meyer et al., 2015; Briner et al., 2016). This study provides a additional insights on Holocene time scales into the regional characteristics of Arctic temperature changes. With the addition of our model analysis this study improves our understanding of the drivers of variability changes in Arctic temperature on centennial and millennial time scales. The role of sea ice and sea level pressure offers an explanation for the regional differences in Arctic temperature trends.

400 The study demonstrates that the asymmetry of the orbital forcing-only simulations is greater than that of the full forcing simulation. Stronger response to orbital forcing implies that the other forcings (e.g. GHG) may compensate this asymmetry. The stronger response to orbital forcing implies that the combined effects of other forcings (e.g., solar irradiance, volcanic eruptions, greenhouse gases, and land use/land cover) and internal climate variability may compensate for the temperature asymmetry pattern. In particular, volcanic eruptions have a larger impact on temperature at a short time scales in region, while

405 the greenhouse gas forcing plays a more critical role as a driver of future climate than orbital forcing. Nevertheless, the individual contribution of each forcing has not been clearly investigated in our study. To fully understand the potential compensation effects induced by volcanic eruption, TSI and GHG forcing, the next steps regarding paleo Arctic temperature studies are compiling more high-resolution, seasonal paleoclimate temperature data, employing and analyzing the results of more comprehensive state-of-the-art simulations of different forcings (e.g. TraCE-21ka (Liu et al., 2014), IPSL (Braconnot et

410 al., 2019)) for reducing the uncertainty of the models and the validation of the roles of different forcing.

5 Summary

The findings from this paper suggests that the Arctic temperature has an asymmetric cooling trend with more cooling over the Atlantic Arctic (-1.54 °C) than the Pacific Arctic (-0.61 °C) during the Holocene, based on Temperature 12k database (Kaufman et al., 2020). In our modeling results, a similar asymmetric change of temperature in the Arctic can be reproduced by CESM,

415 dominated by orbital forcing. Our model simulations show the strongest cooling in the Arctic Ocean, Greenland Island, and the North Atlantic, while the temperature in northern Eurasia and northern Canada shows a warming trend. There is a seasonal

difference in the asymmetric cooling trend, which is dominated by the DJF temperature variability. The Arctic dipole mode of sea level pressure and sea ice play a major role in asymmetric temperature changes. Using no-accelerated simulations to test the robustness of our results the Arctic temperature asymmetry, we found that the ECBilt-CLIO and IPSL simulations are similar to our results, while TraCE-21ka shows the opposite asymmetry.

删除了: Using the non-accelerated model to verify the Arctic temperature asymmetry,

Acknowledgments

This work was jointly supported by the National Natural Science Foundation of China (Grant Nos. 42130604, 42105044, 41971108, 42105044, and 42111530182) and the Priority Academic Program Development of Jiangsu Higher Education Institutions (Grant No. 164320H116). J. Sjolte was supported by the strategic research program of ModEling the Regional and Global Earth system (MERGE) hosted by the Faculty of Science at Lund University. Z. Lu received funding from FORMAS mobility (Grant no. 2020-02267)

References

Aagaard, K. and Carmack, E. C.: The role of sea ice and other fresh water in the Arctic circulation, Journal of Geophysical Research: Oceans, 94, 14485–14498, https://doi.org/10.1029/JC094iC10p14485, 1989.

Alekseev, G. V., Johannessen, O. M., Korablev, A. A., Ivanov, V. V., and Kovalevsky, D. V.: Interannual variability in water masses in the Greenland Sea and adjacent areas, Polar Research, 20, 201–208, https://doi.org/10.1111/j.1751-8369.2001.tb00057.x, 2001.

Bader, J., Jungclaus, J., Krivova, N., Lorenz, S., Maycock, A., Raddatz, T., Schmidt, H., Toohey, M., Wu, C.-J., and Claussen, M.: Global temperature modes shed light on the Holocene temperature conundrum, Nat Commun, 11, 4726, https://doi.org/10.1038/s41467-020-18478-6, 2020.

Barnes, E. A. and Screen, J. A.: The impact of Arctic warming on the midlatitude jet-stream: Can it? Has it? Will it?, WIREs Climate Change, 6, 277–286, https://doi.org/10.1002/wcc.337, 2015.

Berger, A.: Long-Term Variations of Daily Insolation and Quaternary Climatic Changes, Journal of the Atmospheric Sciences, 35, 2362–2367, https://doi.org/10.1175/1520-0469(1978)035<2362:LTVODI>2.0.CO;2, 1978.

Blackport, R. and Kushner, P. J.: The Role of Extratropical Ocean Warming in the Coupled Climate Response to Arctic Sea Ice Loss, Journal of Climate, 31, 9193–9206, https://doi.org/10.1175/JCLI-D-18-0192.1, 2018.

Braconnot, P., Otto-Bliesner, B., Harrison, S., Joussaume, S., Peterchmitt, J.-Y., Abe-Ouchi, A., Crucifix, M., Driesschaert, E., Fichefet, T., Hewitt, C. D., Kageyama, M., Kitoh, A., Loutre, M.-F., Marti, O., Merkel, U., Ramstein, G., Valdes, P., Weber, L., Yu, Y., and Zhao, Y.: Results of PMIP2 coupled simulations of the Mid-Holocene and Last Glacial Maximum – Part 2: feedbacks with emphasis on the location of the ITCZ and mid- and high latitudes heat budget, Climate of the Past, 3, 279–296, https://doi.org/10.5194/cp-3-279-2007, 2007.

Braconnot, P., Zhu, D., Marti, O., and Servonnat, J.: Strengths and challenges for transient Mid- to Late Holocene simulations with dynamical vegetation, Climate of the Past, 15, 997–1024, https://doi.org/10.5194/cp-15-997-2019, 2019.

Briner, J. P., McKay, N. P., Axford, Y., Bennike, O., Bradley, R. S., de Vernal, A., Fisher, D., Francus, P., Fréchette, B., Gajewski, K., Jennings, A., Kaufman, D. S., Miller, G., Rouston, C., and Wagner, B.: Holocene climate change in Arctic Canada and Greenland, Quaternary Science Reviews, 147, 340–364, https://doi.org/10.1016/j.quascirev.2016.02.010, 2016.

Chen, F., Yu, Z., Yang, M., Ito, E., Wang, S., Madsen, D. B., Huang, X., Zhao, Y., Sato, T., John B. Birks, H., Boomer, I., Chen, J., An, C., and Wünnemann, B.: Holocene moisture evolution in arid central Asia and its out-of-phase relationship with Asian monsoon history, Quaternary Science Reviews, 27, 351–364, https://doi.org/10.1016/j.quascirev.2007.10.017, 2008.

Chen, G., Lu, J., Burrows, D. A., and Leung, L. R.: Local finite-amplitude wave activity as an objective diagnostic of midlatitude extreme weather, Geophysical Research Letters, 42, 10,952-10,960, https://doi.org/10.1002/2015GL066959, 2015.

Choi, N., Kim, K.-M., Lim, Y.-K., and Lee, M.-I.: Decadal changes in the leading patterns of sea level pressure in the Arctic and their impacts on the sea ice variability in boreal summer, The Cryosphere, 13, 3007–3021, https://doi.org/10.5194/tc-13-3007-2019, 2019.

Cohen, J.: An observational analysis: Tropical relative to Arctic influence on midlatitude weather in the era of Arctic amplification, Geophysical Research Letters, 43, 5287–5294, https://doi.org/10.1002/2016GL069102, 2016.

Cohen, J., Screen, J. A., Furtado, J. C., Barlow, M., Whittleston, D., Coumou, D., Francis, J., Dethloff, K., Entekhabi, D., Overland, J., and Jones, J.: Recent Arctic amplification and extreme mid-latitude weather, Nature Geosci, 7, 627–637, https://doi.org/10.1038/ngeo2234, 2014.

Cohen, J., Pfeiffer, K., and Francis, J. A.: Warm Arctic episodes linked with increased frequency of extreme winter weather in the United States, Nat Commun, 9, 869, https://doi.org/10.1038/s41467-018-02992-9, 2018.

Dai, H.: Roles of Surface Albedo, Surface Temperature and Carbon Dioxide in the Seasonal Variation of Arctic Amplification, Geophysical Research Letters, 48, e2020GL090301, https://doi.org/10.1029/2020GL090301, 2021.

Delworth, T. L. and Knutson, T. R.: Simulation of Early 20th Century Global Warming, Science, 287, 2246–2250, https://doi.org/10.1126/science.287.5461.2246, 2000.

Deser, C., Tomas, R. A., and Sun, L.: The Role of Ocean–Atmosphere Coupling in the Zonal-Mean Atmospheric Response to Arctic Sea Ice Loss, Journal of Climate, 28, 2168–2186, https://doi.org/10.1175/JCLI-D-14-00325.1, 2015.

Deser, C., Sun, L., Tomas, R. A., and Screen, J.: Does ocean coupling matter for the northern extratropical response to projected Arctic sea ice loss?, Geophysical Research Letters, 43, 2149–2157, https://doi.org/10.1002/2016GL067792, 2016.

Francis, J. and Skific, N.: Evidence linking rapid Arctic warming to mid-latitude weather patterns, Philosophical Transactions of the Royal Society A: Mathematical, Physical and Engineering Sciences, 373, 20140170, https://doi.org/10.1098/rsta.2014.0170, 2015.

Francis, J. A. and Hunter, E.: Drivers of declining sea ice in the Arctic winter: A tale of two seas, Geophysical Research Letters, 34, https://doi.org/10.1029/2007GL030995, 2007.

Francis, J. A. and Vavrus, S. J.: Evidence linking Arctic amplification to extreme weather in mid-latitudes, Geophysical Research Letters, 39, https://doi.org/10.1029/2012GL051000, 2012.

Francis, J. A. and Vavrus, S. J.: Evidence for a wavier jet stream in response to rapid Arctic warming, Environ. Res. Lett., 10, 485   014005, https://doi.org/10.1088/1748-9326/10/1/014005, 2015.

Funder, S., Goosse, H., Jepsen, H., Kaas, E., Kjær, K. H., Korsgaard, N. J., Larsen, N. K., Linderson, H., Lyså, A., Möller, P., Olsen, J., and Willerslev, E.: A 10,000-Year Record of Arctic Ocean Sea-Ice Variability—View from the Beach, Science, 333, 747–750, https://doi.org/10.1126/science.1202760, 2011.

Gajewski, K.: Quantitative reconstruction of Holocene temperatures across the Canadian Arctic and Greenland, Global and 490   Planetary Change, 128, 14–23, https://doi.org/10.1016/j.gloplacha.2015.02.003, 2015.

Gao, C., Ludlow, F., Matthews, J. A., Stine, A. R., Robock, A., Pan, Y., Breen, R., Nolan, B., and Sigl, M.: Volcanic climate impacts can act as ultimate and proximate causes of Chinese dynastic collapse, Commun Earth Environ, 2, 1–11, https://doi.org/10.1038/s43247-021-00284-7, 2021.

Goosse, H. and Fichefet, T.: Importance of ice-ocean interactions for the global ocean circulation: A model study, Journal of 495   Geophysical Research: Oceans, 104, 23337–23355, https://doi.org/10.1029/1999JC900215, 1999.

Grieser, J. and Schonwiese, C.-D.: Parameterization of Spatio-temporal Patterns of Volcanic Aerosol Induced Stratospheric Optical Depth and its Climate Radiative Forcing, Atmósfera, 12, 1999.

Hanslik, D., Jakobsson, M., Backman, J., Björck, S., Sellén, E., O'Regan, M., Fornaciari, E., and Skog, G.: Quaternary Arctic Ocean sea ice variations and radiocarbon reservoir age corrections, Quaternary Science Reviews, 29, 3430–3441, 500   https://doi.org/10.1016/j.quascirev.2010.06.011, 2010.

Hoerling, M. P., Hurrell, J. W., and Xu, T.: Tropical Origins for Recent North Atlantic Climate Change, Science, 292, 90–92, https://doi.org/10.1126/science.1058582, 2001.

Holland, M. M. and Bitz, C. M.: Polar amplification of climate change in coupled models, Climate Dynamics, 21, 221–232, https://doi.org/10.1007/s00382-003-0332-6, 2003.

505   Holton, J. R., Haynes, P. H., McIntyre, M. E., Douglass, A. R., Rood, R. B., and Pfister, L.: Stratosphere-troposphere exchange, Reviews of Geophysics, 33, 403–439, https://doi.org/10.1029/95RG02097, 1995.

Hurrell, J. W.: Decadal Trends in the North Atlantic Oscillation: Regional Temperatures and Precipitation, Science, 269, 676–679, https://doi.org/10.1126/science.269.5224.676, 1995.

Jenkins, M. and Dai, A.: The Impact of Sea-Ice Loss on Arctic Climate Feedbacks and Their Role for Arctic Amplification, 510   Geophysical Research Letters, 48, e2021GL094599, https://doi.org/10.1029/2021GL094599, 2021.

Jennings, A. E., Knudsen, K. L., Hald, M., Hansen, C. V., and Andrews, J. T.: A mid-Holocene shift in Arctic sea-ice variability on the East Greenland Shelf, The Holocene, 12, 49–58, https://doi.org/10.1191/0959683602hl519rp, 2002.

Jing, Y., Liu, J., and Wan, L.: Comparison of climate responses to orbital forcing at different latitudes during the Holocene, Quaternary International, 622, 65–76, https://doi.org/10.1016/j.quaint.2022.02.004, 2022.

515 Johannessen, O. M., Bengtsson, L., Miles, M. W., Kuzmina, S. I., Semenov, V. A., Alekseev, G. V., Nagurnyi, A. P., Zakharov, V. F., Bobylev, L. P., Pettersson, L. H., Hasselmann, K., and Cattle, H. P.: Arctic climate change: observed and modelled temperature and sea-ice variability, Tellus A: Dynamic Meteorology and Oceanography, 56, 328–341, https://doi.org/10.3402/tellusa.v56i4.14418, 2004.

Jones, P. D. and Moberg, A.: Hemispheric and Large-Scale Surface Air Temperature Variations: An Extensive Revision and
520 an Update to 2001, Journal of Climate, 16, 206–223, https://doi.org/10.1175/1520-0442(2003)016<0206:HALSSA>2.0.CO;2, 2003.

Jonkers, L., Cartapanis, O., Langner, M., McKay, N., Mulitza, S., Strack, A., and Kucera, M.: Integrating palaeoclimate time series with rich metadata for uncertainty modelling: strategy and documentation of the PalMod 130k marine palaeoclimate data synthesis, Earth System Science Data, 12, 1053–1081, https://doi.org/10.5194/essd-12-1053-2020, 2020.

525 Joos, F. and Spahni, R.: Rates of change in natural and anthropogenic radiative forcing over the past 20,000 years, PNAS, 105, 1425–1430, https://doi.org/10.1073/pnas.0707386105, 2008.

Kaufman, D., McKay, N., Routson, C., Erb, M., Davis, B., Heiri, O., Jaccard, S., Tierney, J., Dätwyler, C., Axford, Y., Brussel, T., Cartapanis, O., Chase, B., Dawson, A., de Vernal, A., Engels, S., Jonkers, L., Marsicek, J., Moffa-Sánchez, P., Morrill, C., Orsi, A., Rehfeld, K., Saunders, K., Sommer, P. S., Thomas, E., Tonello, M., Tóth, M., Vachula, R., Andreev, A., Bertrand,
530 S., Biskaborn, B., Bringué, M., Brooks, S., Caniupán, M., Chevalier, M., Cwynar, L., Emile-Geay, J., Fegyveresi, J., Feurdean, A., Finsinger, W., Fortin, M.-C., Foster, L., Fox, M., Gajewski, K., Grosjean, M., Hausmann, S., Heinrichs, M., Holmes, N., Ilyashuk, B., Ilyashuk, E., Juggins, S., Khider, D., Koinig, K., Langdon, P., Larocque-Tobler, I., Li, J., Lotter, A., Luoto, T., Mackay, A., Magyari, E., Malevich, S., Mark, B., Massaferro, J., Montade, V., Nazarova, L., Novenko, E., Pařil, P., Pearson, E., Peros, M., Pienitz, R., Płóciennik, M., Porinchu, D., Potito, A., Rees, A., Reinemann, S., Roberts, S., Rolland, N., Salonen,
535 S., Self, A., Seppä, H., Shala, S., St-Jacques, J.-M., Stenni, B., Syrykh, L., Tarrats, P., Taylor, K., van den Bos, V., Velle, G., Wahl, E., Walker, I., Wilmshurst, J., Zhang, E., and Zhilich, S.: A global database of Holocene paleotemperature records, Sci Data, 7, 115, https://doi.org/10.1038/s41597-020-0445-3, 2020.

Kaufman, D. S., Ager, T. A., Anderson, N. J., Anderson, P. M., Andrews, J. T., Bartlein, P. J., Brubaker, L. B., Coats, L. L., Cwynar, L. C., Duvall, M. L., Dyke, A. S., Edwards, M. E., Eisner, W. R., Gajewski, K., Geirsdóttir, A., Hu, F. S., Jennings,
540 A. E., Kaplan, M. R., Kerwin, M. W., Lozhkin, A. V., MacDonald, G. M., Miller, G. H., Mock, C. J., Oswald, W. W., Otto-Bliesner, B. L., Porinchu, D. F., Rühland, K., Smol, J. P., Steig, E. J., and Wolfe, B. B.: Holocene thermal maximum in the western Arctic (0–180°W), Quaternary Science Reviews, 23, 529–560, https://doi.org/10.1016/j.quascirev.2003.09.007, 2004.

Kaufman, D. S., Schneider, D. P., McKay, N. P., Ammann, C. M., Bradley, R. S., Briffa, K. R., Miller, G. H., Otto-Bliesner, B. L., Overpeck, J. T., Vinther, B. M., Arctic Lakes 2k Project Members, Abbott, M., Axford, Y., Bird, B., Birks, H. J. B.,
545 Bjune, A. E., Briner, J., Cook, T., Chipman, M., Francus, P., Gajewski, K., Geirsdóttir, Á., Hu, F. S., Kutchko, B., Lamoureux, S., Loso, M., MacDonald, G., Peros, M., Porinchu, D., Schiff, C., Seppä, H., and Thomas, E.: Recent Warming Reverses Long-Term Arctic Cooling, Science, 325, 1236–1239, https://doi.org/10.1126/science.1173983, 2009.

Kay, J. E., L'Ecuyer, T., Gettelman, A., Stephens, G., and O'Dell, C.: The contribution of cloud and radiation anomalies to the 2007 Arctic sea ice extent minimum, Geophysical Research Letters, 35, https://doi.org/10.1029/2008GL033451, 2008.

550 Klein Goldewijk, K., Beusen, A., Doelman, J., and Stehfest, E.: Anthropogenic land use estimates for the Holocene – HYDE 3.2, Earth System Science Data, 9, 927–953, https://doi.org/10.5194/essd-9-927-2017, 2017.

Kutzbach, J. E., Liu, X., Liu, Z., and Chen, G.: Simulation of the evolutionary response of global summer monsoons to orbital forcing over the past 280,000 years, Clim Dyn, 30, 567–579, https://doi.org/10.1007/s00382-007-0308-z, 2008.

Larsen, N. K., Kjær, K. H., Lecavalier, B., Bjørk, A. A., Colding, S., Huybrechts, P., Jakobsen, K. E., Kjeldsen, K. K., Knudsen,
555 K.-L., Odgaard, B. V., and Olsen, J.: The response of the southern Greenland ice sheet to the Holocene thermal maximum, Geology, 43, 291–294, https://doi.org/10.1130/G36476.1, 2015.

Liu, Z., Otto-Bliesner, B. L., He, F., Brady, E. C., Tomas, R., Clark, P. U., Carlson, A. E., Lynch-Stieglitz, J., Curry, W., Brook, E., Erickson, D., Jacob, R., Kutzbach, J., and Cheng, J.: Transient Simulation of Last Deglaciation with a New Mechanism for Bølling-Allerød Warming, Science, 325, 310–314, https://doi.org/10.1126/science.1171041, 2009.

560 Liu, Z., Lu, Z., Wen, X., Otto-Bliesner, B. L., Timmermann, A., and Cobb, K. M.: Evolution and forcing mechanisms of El Niño over the past 21,000 years, Nature, 515, 550–553, https://doi.org/10.1038/nature13963, 2014.

Lorenz, S. J. and Lohmann, G.: Acceleration technique for Milankovitch type forcing in a coupled atmosphere-ocean circulation model: method and application for the holocene, Climate Dynamics, 23, 727–743, 2004.

Lu, Z. and Liu, Z.: Orbital modulation of ENSO seasonal phase locking, Clim Dyn, 52, 4329–4350,
565 https://doi.org/10.1007/s00382-018-4382-1, 2019.

Malevich, S. B., Vetter, L., and Tierney, J. E.: Global Core Top Calibration of δ18O in Planktic Foraminifera to Sea Surface Temperature, Paleoceanography and Paleoclimatology, 34, 1292–1315, https://doi.org/10.1029/2019PA003576, 2019.

Mandel, I. and Lipovetsky, S.: Climate Change Report IPCC 2021 – A Chimera of Science and Politics, Social Science Research Network, Rochester, NY, https://doi.org/10.2139/ssrn.3913788, 2021.

570 Marcott, S. A., Shakun, J. D., Clark, P. U., and Mix, A. C.: A reconstruction of regional and global temperature for the past 11,300 years, Science, 339, 1198–1201, https://doi.org/10.1126/science.1228026, 2013.

Marsicek, J., Shuman, B. N., Bartlein, P. J., Shafer, S. L., and Brewer, S.: Reconciling divergent trends and millennial variations in Holocene temperatures, Nature, 554, 92–96, https://doi.org/10.1038/nature25464, 2018.

Meyer, H., Opel, T., Laepple, T., Dereviagin, A. Y., Hoffmann, K., and Werner, M.: Long-term winter warming trend in the
575 Siberian Arctic during the mid- to late Holocene, Nature Geosci, 8, 122–125, https://doi.org/10.1038/ngeo2349, 2015.

Müller, J., Werner, K., Stein, R., Fahl, K., Moros, M., and Jansen, E.: Holocene cooling culminates in sea ice oscillations in Fram Strait, Quaternary Science Reviews, 47, 1–14, https://doi.org/10.1016/j.quascirev.2012.04.024, 2012.

Niebauer, H. J., Bond, N., Yakunin, L. P., and Plotnikov, V.: An update on the climatology and sea ice of the Bering Sea, undefined, 1999.

580 Overland, J. E. and Wang, M.: Increased Variability in the Early Winter Subarctic North American Atmospheric Circulation, Journal of Climate, 28, 7297–7305, https://doi.org/10.1175/JCLI-D-15-0395.1, 2015.

Park, H.-S., Kim, S.-J., Seo, K.-H., Stewart, A. L., Kim, S.-Y., and Son, S.-W.: The impact of Arctic sea ice loss on mid-Holocene climate, Nat Commun, 9, 4571, https://doi.org/10.1038/s41467-018-07068-2, 2018.

Polyakov, I. V. and Johnson, M. A.: Arctic decadal and interdecadal variability, Geophysical Research Letters, 27, 4097–4100,
585 https://doi.org/10.1029/2000GL011909, 2000.

Polyakov, I. V., Alekseev, G. V., Bekryaev, R. V., Bhatt, U., Colony, R. L., Johnson, M. A., Karklin, V. P., Makshtas, A. P., Walsh, D., and Yulin, A. V.: Observationally based assessment of polar amplification of global warming, Geophysical Research Letters, 29, 25-1-25–4, https://doi.org/10.1029/2001GL011111, 2002.

Ragner, C.: The 21st Century — Turning Point for the Northern Sea Route?: Proceedings of the Northern Sea Route User
590 Conference, Oslo, 18–20 November 1999, https://doi.org/10.1007/978-94-017-3228-4, 2000.

Rahmstorf, S.: Shifting seas in the greenhouse?, Nature, 399, 523–524, https://doi.org/10.1038/21066, 1999.

Renssen, H., Goosse, H., Fichefet, T., Brovkin, V., Driesschaert, E., Wolk, F., and Climate Change and Landscape Dynamics: Simulating the Holocene climate evolution at northern high latitudes using a coupled atmosphere-sea ice-ocean-vegetation model, Climate Dynamics, 24, 23–43, https://doi.org/10.1007/s00382-004-0485-y, 2005.

595 Renssen, H., Seppä, H., Crosta, X., Goosse, H., and Roche, D. M.: Global characterization of the Holocene Thermal Maximum, Quaternary Science Reviews, 48, 7–19, https://doi.org/10.1016/j.quascirev.2012.05.022, 2012.

Rodionov, S. N., Overland, J. E., and Bond, N. A.: The Aleutian Low and Winter Climatic Conditions in the Bering Sea. Part I: Classification, Journal of Climate, 18, 160–177, https://doi.org/10.1175/JCLI3253.1, 2005.

Routson, C. C., McKay, N. P., Kaufman, D. S., Erb, M. P., Goosse, H., Shuman, B. N., Rodysill, J. R., and Ault, T.: Mid-
600 latitude net precipitation decreased with Arctic warming during the Holocene, Nature, 568, 83–87, https://doi.org/10.1038/s41586-019-1060-3, 2019.

Screen, J. A.: Far-flung effects of Arctic warming, Nature Geosci, 10, 253–254, https://doi.org/10.1038/ngeo2924, 2017.

Screen, J. A. and Simmonds, I.: Amplified mid-latitude planetary waves favour particular regional weather extremes, Nature Clim Change, 4, 704–709, https://doi.org/10.1038/nclimate2271, 2014.

605 Serreze, M. C. and Barry, R. G.: Processes and impacts of Arctic amplification: A research synthesis, Global and Planetary Change, 77, 85–96, https://doi.org/10.1016/j.gloplacha.2011.03.004, 2011.

Sigl, M., Winstrup, M., McConnell, J. R., Welten, K. C., Plunkett, G., Ludlow, F., Büntgen, U., Caffee, M., Chellman, N., Dahl-Jensen, D., Fischer, H., Kipfstuhl, S., Kostick, C., Maselli, O. J., Mekhaldi, F., Mulvaney, R., Muscheler, R., Pasteris, D. R., Pilcher, J. R., Salzer, M., Schüpbach, S., Steffensen, J. P., Vinther, B. M., and Woodruff, T. E.: Timing and climate forcing
610 of volcanic eruptions for the past 2,500 years, Nature, 523, 543–549, https://doi.org/10.1038/nature14565, 2015.

Skeie, P.: Meridional flow variability over the Nordic Seas in the Arctic oscillation framework, Geophysical Research Letters, 27, 2569–2572, https://doi.org/10.1029/2000GL011529, 2000.

Smith, D. M., Screen, J. A., Deser, C., Cohen, J., Fyfe, J. C., García-Serrano, J., Jung, T., Kattsov, V., Matei, D., Msadek, R., Peings, Y., Sigmond, M., Ukita, J., Yoon, J.-H., and Zhang, X.: The Polar Amplification Model Intercomparison Project

615 (PAMIP) contribution to CMIP6: investigating the causes and consequences of polar amplification, Geoscientific Model Development, 12, 1139–1164, https://doi.org/10.5194/gmd-12-1139-2019, 2019.

Smith, R. S. and Gregory, J.: The last glacial cycle: transient simulations with an AOGCM, Clim Dyn, 38, 1545–1559, https://doi.org/10.1007/s00382-011-1283-y, 2012.

Stabeno, P. J., Bond, N. A., Kachel, N. B., Salo, S. A., and Schumacher, J. D.: On the temporal variability of the physical
620 environment over the south-eastern Bering Sea, Fisheries Oceanography, 10, 81–98, https://doi.org/10.1046/j.1365-2419.2001.00157.x, 2001.

Sundqvist, H. S., Kaufman, D. S., McKay, N. P., Balascio, N. L., Briner, J. P., Cwynar, L. C., Sejrup, H. P., Seppä, H., Subetto, D. A., Andrews, J. T., Axford, Y., Bakke, J., Birks, H. J. B., Brooks, S. J., de Vernal, A., Jennings, A. E., Ljungqvist, F. C., Rühland, K. M., Saenger, C., Smol, J. P., and Viau, A. E.: Arctic Holocene proxy climate database – new approaches
625 to assessing geochronological accuracy and encoding climate variables, Climate of the Past, 10, 1605–1631, https://doi.org/10.5194/cp-10-1605-2014, 2014.

Tierney, J. E. and Tingley, M. P.: A Bayesian, spatially-varying calibration model for the TEX86 proxy, Geochimica et Cosmochimica Acta, 127, 83–106, https://doi.org/10.1016/j.gca.2013.11.026, 2014.

Tierney, J. E. and Tingley, M. P.: BAYSPLINE: A New Calibration for the Alkenone Paleothermometer, Paleoceanography
630 and Paleoclimatology, 33, 281–301, https://doi.org/10.1002/2017PA003201, 2018.

Tierney, J. E., Malevich, S. B., Gray, W., Vetter, L., and Thirumalai, K.: Bayesian Calibration of the Mg/Ca Paleothermometer in Planktic Foraminifera, Paleoceanography and Paleoclimatology, 34, 2005–2030, https://doi.org/10.1029/2019PA003744, 2019.

Timm, O. and Timmermann, A.: Simulation of the Last 21 000 Years Using Accelerated Transient Boundary Conditions*,
635 Journal of Climate, 20, 4377–4401, https://doi.org/10.1175/JCLI4237.1, 2007.

Timmermann, A., Friedrich, T., Timm, O. E., Chikamoto, M. O., Abe-Ouchi, A., and Ganopolski, A.: Modeling Obliquity and CO2 Effects on Southern Hemisphere Climate during the Past 408 ka, Journal of Climate, 27, 1863–1875, https://doi.org/10.1175/JCLI-D-13-00311.1, 2014.

Varma, V., Prange, M., Merkel, U., Kleinen, T., Lohmann, G., Pfeiffer, M., Renssen, H., Wagner, A., Wagner, S., and Schulz,
640 M.: Holocene evolution of the Southern Hemisphere westerly winds in transient simulations with global climate models, Climate of the Past, 8, 391–402, https://doi.org/10.5194/cp-8-391-2012, 2012.

Vavrus, S. J.: The Influence of Arctic Amplification on Mid-latitude Weather and Climate, Curr Clim Change Rep, 4, 238–249, https://doi.org/10.1007/s40641-018-0105-2, 2018.

de Vernal, A., Hillaire-Marcel, C., and Darby, D. A.: Variability of sea ice cover in the Chukchi Sea (western Arctic Ocean)
645 during the Holocene: HOLOCENE SEA ICE IN THE CHUKCHI SEA, Paleoceanography, 20, n/a-n/a, https://doi.org/10.1029/2005PA001157, 2005.

Vieira, L. E. A., Solanki, S. K., Krivova, N. A., and Usoskin, I.: Evolution of the solar irradiance during the Holocene, A&A, 531, A6, https://doi.org/10.1051/0004-6361/201015843, 2011.

Wan L., Jian L., Chaochao G., Weiyi S., Liang N., and Mi Y.: Study about influence of the Holocene volcanic eruptions on

650   temperature variation trend by simulation, Quaternary Sciences, 40, 1597–1610, https://doi.org/10.11928/j.issn.1001-
7410.2020.06.19, 2020.

Wang, J. and Ikeda, M.: Arctic oscillation and Arctic sea-ice oscillation, Geophysical Research Letters, 27, 1287–1290,
https://doi.org/10.1029/1999GL002389, 2000.

Wanner, H., Solomina, O., Grosjean, M., Ritz, S. P., and Jetel, M.: Structure and origin of Holocene cold events, Quaternary

655   Science Reviews, 30, 3109–3123, https://doi.org/10.1016/j.quascirev.2011.07.010, 2011.

Watanabe, E., Wang, J., Sumi, A., and Hasumi, H.: Arctic dipole anomaly and its contribution to sea ice export from the Arctic
Ocean in the 20th century, Geophysical Research Letters, 33, https://doi.org/10.1029/2006GL028112, 2006.

Wohlfahrt, J., Harrison, S. P., and Braconnot, P.: Synergistic feedbacks between ocean and vegetation on mid- and high-
latitude climates during the mid-Holocene, Climate Dynamics, 22, 223–238, https://doi.org/10.1007/s00382-003-0379-4, 2004.

660   Wu, B., Wang, J., and Walsh, J.: Possible Feedback of Winter Sea Ice in the Greenland and Barents Seas on the Local
Atmosphere,   Monthly   Weather   Review,   132,   1868–1876,   https://doi.org/10.1175/1520-
0493(2004)132<1868:PFOWSI>2.0.CO;2, 2004.

Wu, B., Wang, J., and Walsh, J. E.: Dipole Anomaly in the Winter Arctic Atmosphere and Its Association with Sea Ice Motion,
Journal of Climate, 19, 210–225, https://doi.org/10.1175/JCLI3619.1, 2006.

665   Xue, D., Lu, J., Sun, L., Chen, G., and Zhang, Y.: Local increase of anticyclonic wave activity over northern Eurasia under
amplified Arctic warming, Geophysical Research Letters, 44, 3299–3308, https://doi.org/10.1002/2017GL072649, 2017.

Zhong, Y., Jahn, A., Miller, G. H., and Geirsdottir, A.: Asymmetric Cooling of the Atlantic and Pacific Arctic During the Past
Two Millennia: A Dual Observation-Modeling Study, Geophys. Res. Lett., 45, https://doi.org/10.1029/2018GL079447, 2018.